

## RESEARCH ARTICLE

# Development of a novel epoxy resin based on epoxidized chia oil as matrix and maleinized chia oil as bio-renewable crosslinker

Ivan Dominguez-Candela<sup>1</sup>  | Aina Perez-Nakai<sup>2</sup> | Elena Torres-Roca<sup>3</sup> | Jaime Lora-Garcia<sup>1</sup> | Vicent Fombuena<sup>2</sup>

<sup>1</sup>Instituto de Seguridad Industrial, Radiofísica y Medioambiental (ISIRYM), Universitat Politècnica de València (UPV), Alcoy, Spain

<sup>2</sup>Technological Institute of Materials (ITM), Universitat Politècnica de València (UPV), Alcoy, Spain

<sup>3</sup>Textile Industry Research Association (AITEK), Alcoy, Spain

## Correspondence

Ivan Dominguez-Candela, Instituto de Seguridad Industrial, Radiofísica y Medioambiental (ISIRYM), Universitat Politècnica de València (UPV), Plaza Ferrándiz y Carbonell, s/n 03801 Alcoy, Spain.  
Email: [ivdocan@doctor.upv.es](mailto:ivdocan@doctor.upv.es)

## Funding information

Ministry of Science and Innovation, Grant/Award Number: PID2020-119142RA-I00; Universitat Politècnica de València, Grant/Award Number: PAID-2019-SP20190013; Generalitat Valenciana, Grant/Award Number: ACIF/2020/233

## Abstract

In this work novel thermosetting resins with high bio-based content have been developed derived from chia seed oil (CO). Epoxidized chia seed oil (ECO) was used as bio-based epoxy matrix with different mixtures of crosslinker agents, that is, methyl nadic anhydride (MNA) as petroleum-derived and maleinized chia seed oil (MCO) as bio-based crosslinker. The chemically modified oils from CO, that is, ECO and MCO, and MNA were analyzed by titration and FT-IR. Additional <sup>1</sup>H NMR analysis was performed to characterize MCO structure. Two different behaviors were observed using the mixtures of crosslinkers. On one hand, MNA increases the rigidity with bio-based content of 54.2%. On the other hand, the addition of MCO provides higher ductility with bio-based content up to 98%. The same trend was observed by DMTA analysis. The novel cured resins were successfully crosslinked as demonstrated by the mechanical properties, FT-IR analyses, and gel content. Based on the results, it is concluded that MCO presents higher reactivity than MNA, decreasing curing time with possible energy saving at industrial level. In general, the results showed that adding the appropriate amount of MCO, green thermosetting resins with the desired thermal and mechanical properties can be manufactured with high bio-based content.

## KEYWORDS

bio-based epoxy resin, chia seed oil, curing time, ductility, epoxidized chia seed oil, maleinized chia seed oil

## 1 | INTRODUCTION

Currently, there is an urgent need to develop innovative technologies and materials from renewable resources in order to reduce dependence on fossil resources. The

current inflation that has led to a sharp increase in the prices of goods and services, together with the current energy crisis, exacerbated by the war in Ukraine, has further highlighted the need for a change in the production model.<sup>1,2</sup> For years, the scientific community

This is an open access article under the terms of the [Creative Commons Attribution-NonCommercial-NoDerivs](https://creativecommons.org/licenses/by-nc-nd/4.0/) License, which permits use and distribution in any medium, provided the original work is properly cited, the use is non-commercial and no modifications or adaptations are made.

© 2022 The Authors. *Journal of Applied Polymer Science* published by Wiley Periodicals LLC.

has been focusing on the need to develop polymeric materials from biomass or plant derivatives, such as starch,<sup>3</sup> cellulose,<sup>4</sup> lignin,<sup>5</sup> marine resources,<sup>6</sup> lipids<sup>7</sup> and vegetable oils (VO),<sup>8</sup> in as much as the utilization of renewable raw materials is one of the 12 Principles of Green Chemistry.<sup>9</sup> This is evidenced by the large number of publications related to materials developed from these precursors.

Of all these renewable precursors, the use of VO is worth highlighting. These have a series of advantages and physicochemical properties that make them particularly interesting in the development of new eco-efficient materials.<sup>10,11</sup> First, they can act as precursors for the development of an infinite number of new products for engineering use, such as cosmetic products and shampoos,<sup>12</sup> lubricants,<sup>13</sup> plasticizers,<sup>14</sup> emulsifiers,<sup>15</sup> or even new thermoset polymers<sup>16</sup> as will be detailed in the current study. Moreover, current data on the production of vegetable oils show their increased production, abundant availability, and relatively low price compared to other precursors obtained from biomass.<sup>17</sup>

The main constituent of the VO are triglycerides, which are the product of the esterification of three fatty acids and glycerol. These fatty acids can be classified according to the number of unsaturations (C=C double bonds), giving rise to saturated fatty acids (SFAs), for example, palmitic acid, monounsaturated fatty acids (MUFAs), such as oleic acid, or polyunsaturated fatty acids (PUFAs), such as linolenic acid. The average value of unsaturations can be expressed in terms of the iodine value (IV) ( $\text{g I}_2 \cdot 100 \text{ g}^{-1}$ ). Therefore, according to this parameter, those oils with IV higher than 100–150, known as drying oils, will be those of greatest industrial interest.<sup>18</sup> This justifies that oils from linseed,<sup>19</sup> soybean,<sup>20</sup> hemp,<sup>21</sup> or tung<sup>22</sup> are the most commonly used in industrial applications. However, it is worth noting that one of the VO with the highest IV, chia seed oil (CO) (*Salvia hispanica L.*), with a value of over  $190 \text{ g I}_2 \cdot 100 \text{ g}^{-1}$ ,<sup>23</sup> and a market with a growth rate of over 23% between 2019 and 2025,<sup>24</sup> has hardly any bibliography related to its possible industrial applications.

For the aforementioned industrial applications, especially in the preparation of polymeric materials, it is necessary to take advantage of the double bonds (C=C) as reactive sites, to cause a functionalization of the triglycerides. In the specific case of thermosetting polymers, these reactive sites act as crosslinking points of the tridimensional chain. Some of these chemical modifications are epoxidation and maleinization. During epoxidation, the double bonds present in the triglycerides are oxidized generating oxirane groups.<sup>25</sup> Current literature shows a wide market for its use as a plasticizer and stabilizer of Poly(vinyl chloride) (PVC)<sup>26–29</sup> and a new opportunity

for the development of bio-based thermosetting epoxy resins.<sup>30</sup>

Besides, to convert VO into a curable thermosetting matrix, the addition of a hardener acting as a curing agent is necessary. The most employed hardeners in epoxy-type resins are anhydrides, and amines.<sup>31</sup> Many works have been developed using different epoxidized VOs such as linseed,<sup>32</sup> soybean,<sup>33</sup> or hemp seed oil<sup>34</sup> crosslinked with petrochemical-based hardeners. Nevertheless, different studies show the toxicity of aliphatic-, cycloaliphatic- and aromatic-amines, as well as the relationship between sensitization and asthma problems related to anhydrides (methyl tetrahydrophthalic anhydride [MTHPA], or tetrahydrophthalic anhydride [THPA] among others).<sup>35,36</sup> However, fewer works have been reported using epoxy resin and bio-based hardeners from VOs. For instance, Stemmelen et al.<sup>37</sup> studied the curing process of epoxidized linseed oil (ELO) as epoxy resin and aminated grapeseed oil (AGSO) as an alternative bio-crosslinker. Other study carried out by the same author was the ELO crosslinked with fatty amides from VOs.<sup>38</sup> Another proposal of bio-based crosslinker is the maleinization of VOs, which consists of the reaction of maleic anhydride (MA) with a double bond, that allows the development of thermosetting resins derived almost entirely from VOs.<sup>39</sup> Takahashi et al.<sup>40</sup> characterized commercial epoxidized soybean oil (ESO) crosslinked with maleinized linseed oil (MLO), obtaining by DTMA a value of glass transition temperature ( $T_g$ ) of  $-41^\circ\text{C}$ . Samper et al.<sup>41</sup> and Fombuena et al.<sup>30</sup> developed thermoset resins based on ESO and composites based on ELO and flax fabrics as reinforcement respectively using mixtures of MNA and MLO as crosslinker agents. Therefore, the use of MLO has been studied previously but, to the best of our knowledge, there is no bibliography related to the oil with the highest unsaturation, CO.

Thus, the overall objective of this study is to develop and optimize novel thermosetting resins obtained from the use of epoxidized chia oil (ECO) as matrix and maleinized chia oil (MCO) as hardener to reach high bio-based content. Different amounts of crosslinker in combination with an anhydride of petrochemical origin, methyl nadic anhydride (MNA), have been systematically varied to test a wide range of thermo-mechanical properties of the new thermoset resin.

## 2 | EXPERIMENTAL

### 2.1 | Materials

In order to obtain thermosetting resins with high bio-based content, two modifications of CO were carried out.

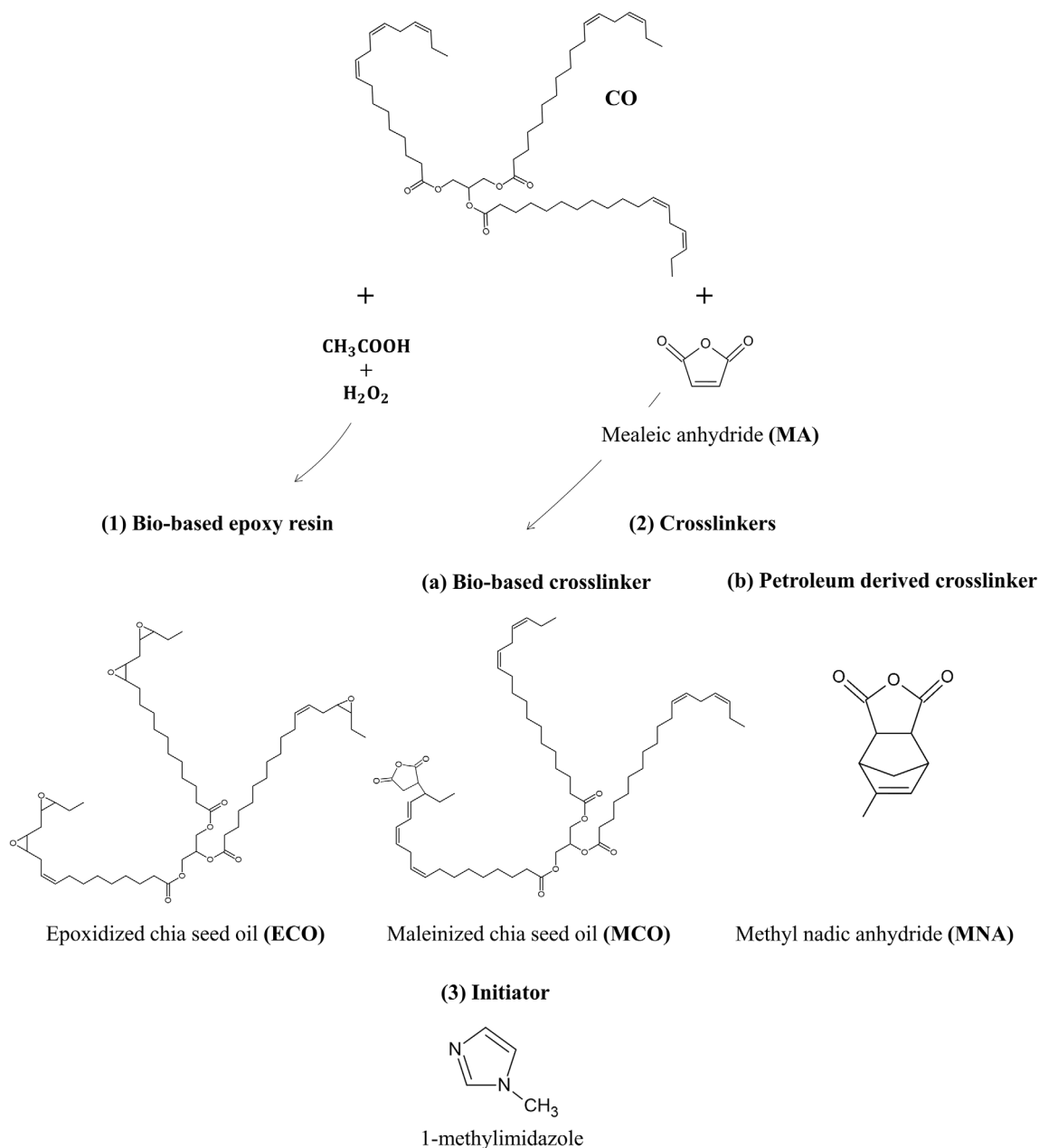


**FIGURE 1** Monomer preparation and chemical structure of bio-based epoxy resin, crosslinkers and initiator. Note that only generous addition of maleic anhydride in MCO is shown, but various modes can take place.

First, CO was extracted from chia seed provided by Fru-toseco (Bigastro, Alicante, Spain). This extraction was performed by cold mechanical extrusion using a CRZ-309 press machine (Changyouxin Trading Co., Zhucheng, China). Afterward, CO was chemically modified by epox- idation and maleinization processes to introduce reactive points in fatty acid chains. The epoxidation of CO was carried out using a molar ratio of hydrogen peroxide: acetic acid: double bond ( $\text{H}_2\text{O}_2:\text{CH}_3\text{COOH}:\text{DB}$ ) of 2:0.5:1 following the procedure described in previous report.<sup>42</sup> ECO was used as epoxy matrix with an epoxy equivalent weight (EEW) of  $219 \text{ g-equiv}^{-1}$  and an iodine value

(IV) of  $19.8 \text{ g I}_2 \cdot 100 \text{ g}^{-1}$ . Two different crosslinkers were added to ECO epoxy matrix.

On one hand, MCO was performed by the maleiniza- tion process adding MA with purity >98% (Sigma Aldrich, Madrid, Spain) to CO. The process was carried out following the methodology described by Lerma-Canto et al.<sup>43</sup> as follows: 300 g of CO was introduced in a three-neck round flask heated up to  $180^\circ\text{C}$  with a constant stirring rate of 200 rpm. First, 9 g of MA per 100 g of CO was added to the round flask for 1 h at constant stirring rate. The same proce- dure was carried out at 200 and  $220^\circ\text{C}$  each hour, with a total reaction time of 3 h. Finally, MCO was cooled down to

room temperature and centrifuged at 4000 rpm for 10 min in order to allow the separation of possible unreacted MA. As result, MCO presented an acid value content of 120 g-equiv<sup>-1</sup> and IV of 104 g I<sub>2</sub>·100 g<sup>-1</sup>. This product was used as bio-based crosslinker to substitute by a petrochemical derived, hence increasing the bio-based content.

On the other hand, MNA supplied by Sigma Aldrich (Madrid, Spain) was used as petrochemical crosslinker. MNA has an anhydride equivalent weight (AEW) of 178.2 g-equiv<sup>-1</sup>. Additionally, the initiator of crosslinking reaction was 1-methyl imidazole (99%), supplied by Sigma Aldrich (Madrid, Spain). This initiator is widely used for anhydride epoxy resins in order to promote the reaction.<sup>44</sup> In this case, 2 wt.% respect to a mixture of both ECO and crosslinker was added as is recommended in the literature.<sup>45</sup> All chemical structures are gathered in Figure 1.

## 2.2 | Characterization of raw materials

The main functional groups of raw materials were identified by Fourier Transform Infrared (FT-IR) spectrophotometer. Samples were spread on the KBr windows and analyzed in a Bruker Vector 22 (Bruker Española S.A, Madrid, Spain). FT-IR spectra was recorded using a range of 4000–400 cm<sup>-1</sup>, averaging 20 scans with 4 cm<sup>-1</sup> resolution.

<sup>1</sup>H NMR was employed to confirm the chemical structure of novel bio-based crosslinker. <sup>1</sup>H NMR spectra of MCO was recorded on a Bruker AMX 500 unit (Bruker BioSpin GmbH, Rheinstetten, Germany) at 25°C. The sample was dissolved in 0.6 ml using deuterated chloroform as solvent and mixed for 10 s. Subsequently, dissolution was transferred to 5 mm NMR tubes for data acquisition.

The iodine value (IV) is an index that indicates the amount of double bonds available in fatty acid chains. The IV was determined by titration process using sodium thiosulfate solution following the guidelines of ISO 3961.

The oxirane oxygen content and epoxy equivalent weight (EEW) measured in % and grams of resin containing 1 g equivalent of epoxy groups, respectively, indicates the conversion of double bonds to epoxy groups within fatty acid chains of vegetable oil. Both values were obtained for ECO by means of CH<sub>3</sub>COOH-HBr titration process using ASTM D1652

The acid value is used to evaluate the maleinization process of MCO and the measurement was carried out by KOH standard solution as is indicated in ISO 660:2009.

## 2.3 | Preparation of samples

The samples were prepared using a formulation ratio EEW:AEW of 1:1 due to this relationship shows a

stoichiometric equilibrium between reactive points and balanced properties in a similar system based on ESO and anhydride crosslinkers.<sup>46</sup> ECO was mixed with different proportions of crosslinkers (MNA and MCO) according to percentage of molar ratio as gathered the Table 1. The mixture was mechanically mixed at room temperature with an intensive mixer (Brabender Instruments Co. Germany) at 100 rpm for 10 min to ensure good mixing. Afterward, 1-methyl imidazole was added to the mixture and mixed until a homogeneous mixture of all components were obtained. The mixtures were placed in silicone molds with dimensions of 80 × 10 × 4 mm<sup>3</sup> and the curing cycle was carried out at 90°C for 3 h followed by post-curing at 130°C for 1 extra hour in an air oven model Conterm 80 L from J. P Selecta (Barcelona, Spain).

## 2.4 | Characterization of the curing process

Dynamic differential scanning calorimetry (DSC) was used in order to study the curing process of the different combinations of resin-hardeners developed. The calorimetric analysis was performed using Mettler-Toledo DSC 821 (Mettler-Toledo, Schwerzenbach, Switzerland). The samples used were in the range of 4–6 mg and were underwent to dynamic program from 30 to 300°C at heating rate of 10°C min<sup>-1</sup>. All experiments were carried out in a nitrogen atmosphere with a constant flow at 66 ml min<sup>-1</sup>.

In addition, isothermal curing of samples was also tested by plate-plate oscillatory rheometer using AR-G2 (TA Instrument, New Castle) equipped with two parallel plates (*D* = 25 mm). The analysis was conducted using isothermal temperature of 90°C until sample was fully cured. The maximum deformation (*γ*) and frequency were set to 0.1% and 1 Hz, respectively, in order to assess the evolution of the phase angle (*δ*).

## 2.5 | Gel content

The cured samples were soaked in acetone as solvent according to literature.<sup>47</sup> Samples were initially weighed (*w*<sub>0</sub>), around 1.5 g by sample, and were subjected to Soxhlet extraction to examine any unreacted resin. All extractions were conducted for 24 h and subsequently dried overnight at 60°C. Each sample was performed by triplicate. The dried sample (*w*<sub>f</sub>) was weighted, and gel content was calculated using the next equation:

$$\text{Gel content (\%)} = \frac{w_f}{w_0} \cdot 100$$

**TABLE 1** Mixture percentages of ECO crosslinked with different proportions of MNA and MCO

Sample	MNA (%)	MCO (%)	Bio-based content (%)
MNA100	100	0	54.2
MNA70:MCO30	70	30	69.4
MNA50:MCO50	50	50	78.5
MNA30:MCO70	30	70	86.8
MCO100	0	100	98.0

## 2.6 | FTIR

Fourier-transformed infrared spectroscopy (FT-IR) equipped with a single reflection attenuated total reflectance (ATR) accessory with a diamond ATR crystal (Madison, Wisconsin) was performed for cured samples. The wavelength range was 4000–600  $\text{cm}^{-1}$  with a spectral resolution of 4  $\text{cm}^{-1}$  and 12 scans. All FT-IR spectra were normalized by using the Perkin-Elmer software Spectrum.

## 2.7 | Mechanical characterization

Mechanical characterization of the different resins developed were studied through flexural, hardness and Charpy impact tests. The flexural tests were conducted on a universal testing machine model ELIB 30 from S.A.E. Ibertest (Madrid, Spain) according to standard ISO 178. A fixed crosshead rate of 5  $\text{mm min}^{-1}$  and load cell of 5 kN were set.

Regarding the impact tests, these were carried out using a 6 J Charpy pendulum (Metrotec S.A., San Sebastián, Spain) according to the guidelines of the ISO 179. Sample sizes of  $80 \times 10 \times 4 \text{ mm}^3$  were used in both flexural and Charpy impact tests. The hardness tests were performed using a Shore D Durometer model 673-D from J. Bolt Instruments (Barcelona, Spain) as indicated by ISO 868. At least five samples were tested at room temperature for each characterization test and the average values were calculated.

Dynamic mechanical thermal analysis (DMTA) was carried out in an oscillatory rheometer AR-G2 (TA Instruments, New Castle). Samples with a sample size of  $36 \times 0.6 \times 0.25 \text{ mm}^3$ , were subjected to torsion-shear mode with a thermal program from  $-20$  to  $100^\circ\text{C}$  at a heating rate of  $10^\circ\text{C/min}$ . The maximum shear deformation ( $\gamma$ ) and frequency were set at 0.1% and 1 Hz, respectively.

## 2.8 | Field emission scanning electron microscopy (FESEM)

The morphologies of fractured samples from impact tests were evaluated for each formulation. A field emission

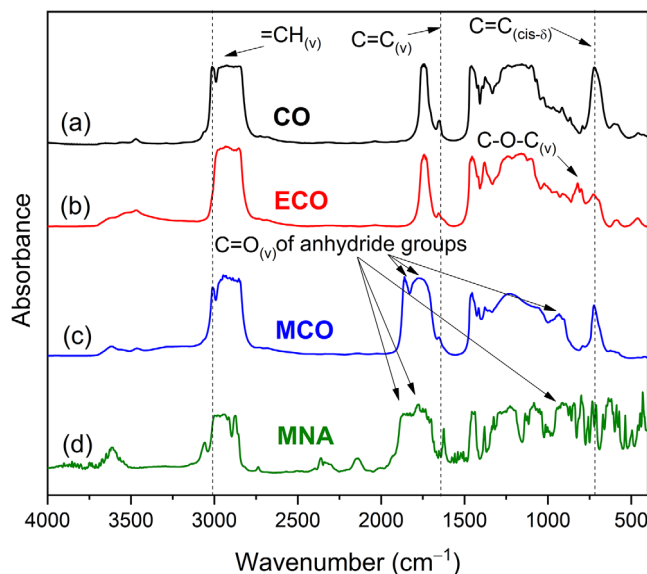


**FIGURE 2** Fourier transform infrared (FT-IR) spectrum of raw materials: (a) CO, (b) ECO, (c) MCO, and (d) MNA [Color figure can be viewed at [wileyonlinelibrary.com](http://wileyonlinelibrary.com)]

scanning electron microscopy (FESEM) with a Zeiss Ultra 55 from Oxford Instruments (Abingdon, UK) was used. Previously to place in FESEM vacuum chamber, sample surfaces were coated with gold-palladium alloy under vacuum conditions using a sputter coater EM MED020 (Leica Microsystems, Wetzlar, Germany). The acceleration voltage applied to electron beam was 2 kV.

## 3 | RESULTS AND DISCUSSION

### 3.1 | Functional group analysis of raw materials

The novel epoxy resin and crosslinker from modified CO, ECO and MCO, as well as MNA were subjected to qualitative characterization by means of FT-IR and quantitative by titration method. In the case of the novel MCO as bio-based crosslinker, H-NMR analysis was performed to corroborate the maleated groups formation. The FTIR spectrums of raw materials are depicted in Figure 2 to identify the main reactive points. First, the Figure 2a



shows the unmodified CO taking as a basis for subsequent chemical modifications. In the CO spectra, the characteristic peaks of double bonds are located at  $3010\text{ cm}^{-1}$  caused by stretching of cis-olefinic bonds ( $=\text{CH}_{(v)}$ ),  $1652\text{ cm}^{-1}$  due to stretching of disubstituted cis-olefins ( $\text{C}=\text{C}_{(v)}$ ) and  $723\text{ cm}^{-1}$  for the combination of rocking vibration and out of plane deformation in cis-disubstituted olefins ( $\text{C}=\text{C}_{(cis-\delta)}$ ). In the ECO spectrum (Figure 2b), the almost disappearance of double bonds peaks particularly at  $3010$  ( $=\text{CH}_{(v)}$ ) and  $723\text{ cm}^{-1}$  ( $\text{C}=\text{C}_{(cis-\delta)}$ ) compared to CO, confirming that the epoxidation process took place. As result, the characteristic ( $\text{C}-\text{O}-\text{C}_{(v)}$ ) stretching peak at  $821\text{ cm}^{-1}$  appeared and was associated to oxirane oxygen group,<sup>48</sup> providing evidence that double bonds were replaced by oxirane oxygen group.

Regarding MCO, the FTIR spectra is plotted in Figure 2c. The maleinization process can follow several paths: the most common is -ene reaction for the addition of MA where unsaturation remains, even though Diels-Alder condensation can be also proceeded in some cases when conjugated carbon-carbon double bonds are present in fatty acid chains.<sup>49</sup> As can be observed in Figure 2c, the peaks of double bonds decreased, probably due to Diels-Alder condensation when conjugated double bonds are formed through -ene reaction. It should point out that CO presents high availability of double bonds in triglyceride (average of 2.24 per each fatty acid from  $^1\text{H NMR}$ )<sup>23</sup> with IV of  $196\text{ g I}_2\cdot 100\text{ g}^{-1}$ , thus there is probability that Diels-Alder condensation reaction takes place. The characteristic peaks associated to the addition of anhydride groups are observed at  $1859$  and  $1781\text{ cm}^{-1}$  corresponding to symmetric and asymmetric vibrations of carbonyl ( $\text{C}=\text{O}_{(v)}$ ), respectively. Furthermore, it should be mentioned that band at  $1859\text{ cm}^{-1}$  was an overtone of  $918\text{ cm}^{-1}$ , which are related to the structure of five carbon of succinic anhydride.<sup>50</sup> In addition, the wider band between  $1800\text{--}1700\text{ cm}^{-1}$  regarding unmodified CO also corresponds to MA moiety that is attached to fatty acid chains.

The petroleum derived crosslinker MNA (Figure 2d), showed a shift of the peak from  $3010$  to  $3050\text{ cm}^{-1}$  ( $=\text{CH}_{(v)}$ ), whereas peaks at  $1652$  ( $\text{C}=\text{C}_{(v)}$ ) and  $723\text{ cm}^{-1}$  ( $\text{C}=\text{C}_{(cis-\delta)}$ ) remained in the same position. The three peaks were observed due to double bond within structure, as was observed in the previous raw materials. Besides, symmetric and asymmetric vibration of ( $\text{C}=\text{O}_{(v)}$ ) was also detected at  $1859$  and  $1781\text{ cm}^{-1}$ , respectively, as well as the presence of peak at  $918\text{ cm}^{-1}$  similar to anhydride group in MCO, being the reactive points that are readily to react with both ECO and MCO.

As a further characterization of MCO as novel bio-based crosslinker,  $^1\text{H NMR}$  spectroscopy was carried out to confirm the formation of maleated groups onto

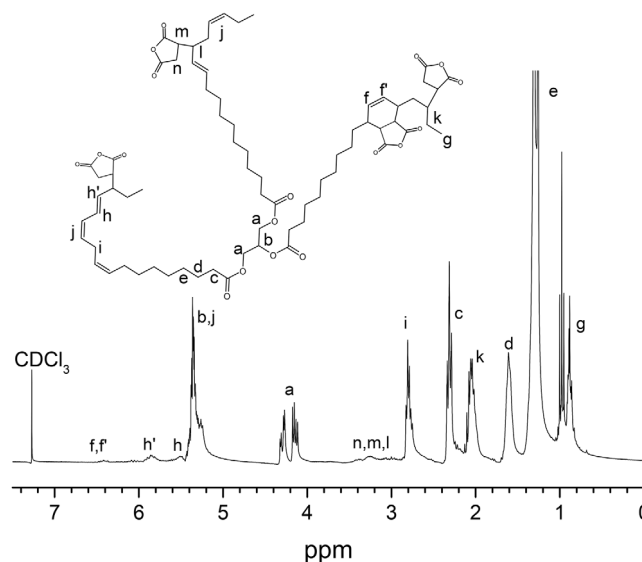
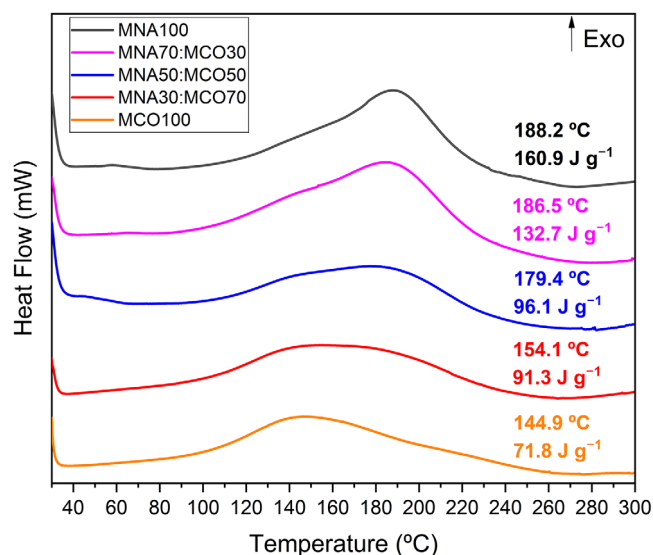


FIGURE 3  $^1\text{H NMR}$  spectra of novel bio-based crosslinker (MCO) with possible types of MA incorporation

triglyceride structure. As can be seen in Figure 3, the signal intensity observed at  $2.8\text{--}3.2\text{ ppm}$  is attributed to methine and methylene protons of succinic groups on MCO structure, confirming the formation of maleated groups. As aforementioned, -ene reaction and Diels-Alder condensation can take place, appearing peaks between  $5.5\text{--}6.5\text{ ppm}$  that correspond to conjugated double bonds formed during -ene reaction and double bonds of Diels-Alder condensation as a consequence of -ene reaction.<sup>51</sup> Therefore, the possible incorporation types of MA on MCO structure are shown in Figure 3. In addition, the residual MA can be also followed with  $^1\text{H NMR}$  spectroscopy at  $7.03\text{ ppm}$ , where any peak was observed.

Regarding MA grafting, an estimation can be obtained by considering the reactions supposed. Taking into account that the conversion of the double bonds is  $45.9\%$  and the average of double bonds present in the CO structure is  $6.72$ , a value approximated of  $3.15$  maleated groups per triglyceride are obtained. However, the analysis done by the  $^1\text{H NMR}$  spectra showed an average content of maleated groups of  $1.1$  in the MCO (Figure 3). This value of  $1.1$  maleated groups per triglyceride is in agreement with the values obtained in previous studies<sup>52</sup> and very close to the  $1.35$  present in commercial MLO.<sup>53</sup> According to the study carried out by Amos et al.,<sup>54</sup> it was concluded that during maleinized reaction exists a competition between the degradation of the MA functionalities and the addition of MA to double bonds, which could be the reason for this lower yield reaction. With this approximation of  $1.1$  maleate groups per triglyceride and with an average molecular weight of  $936\text{ g}\cdot\text{mol}^{-1}$ , the resulting AEW is around  $841\text{ g}\cdot\text{equi}^{-1}$ .



**FIGURE 4** Differential scanning calorimetry (DSC) of ECO crosslinked with different MNA:MCO mixtures at  $10^{\circ}C\ min^{-1}$  [Color figure can be viewed at [wileyonlinelibrary.com](http://wileyonlinelibrary.com)]

Regarding the values obtained by titration methods, the IV of the unmodified CO was found to be  $196\ g\ I_2 \cdot 100\ g^{-1}$ . These elevated value of unsaturations are related to fatty acid composition of CO, which were reported in previous study.<sup>23</sup> Briefly, the most representative fatty acids are: monounsaturated integrated by oleic acid (4.32%) and polyunsaturated such as Linoleic (15.8%) and Linolenic (68.6%) which provide the most double bonds with 2 and 3 double bonds per each fatty acid, respectively. These results show the high availability of the double bonds to react further in epoxidation and maleinization reactions. In the ECO sample, the IV obtained decreased to  $19.8\ g\ I_2 \cdot 100\ g^{-1}$ , confirming that the epoxidation process took place during the chemical modification of the oil. On the other hand, to corroborate if this decrease in the availability of the double bonds is due to the additions of epoxy groups, the EEW and the oxirane oxygen content were determined. Values of  $219\ g \cdot equiv^{-1}$  for the EEW and 7.27% for the oxirane oxygen content confirmed that the introduction of epoxy groups in the CO has been carried out successfully. In the case of MCO, the maleinization reaction also decreased the availability of the double bonds, giving a result of  $104\ g\ I_2 \cdot 100\ g^{-1}$ .

### 3.2 | Characterization of the curing process

In a first stage, the curing process of novel epoxy resins based on ECO was evaluated by dynamic scanning

calorimetry (DSC). The characteristic exothermic peak (Figure 4) provides information regarding the crosslinking reaction between epoxy resin and crosslinker employed, where the main calorimetric values, that is, the temperature of the exothermic curing peak ( $T_p$ ) ( $^{\circ}C$ ), representative of the maximum crosslinking rate of the molecules, and normalized enthalpy ( $J\ g^{-1}$ ), are also gathered. As it can be observed, the crosslinking process of ECO with MNA (MNA100 sample) starts around  $80^{\circ}C$  and ends in the range of  $230\text{--}240^{\circ}C$ , where the  $T_p$  was observed at  $188.2^{\circ}C$ . This exothermic peak is attributed to ring opening reaction between both epoxy groups of ECO and anhydride groups of crosslinkers. Furthermore, this peak is related to reactivity of the compounds in curing process as has been reported by Chen et al.<sup>55</sup> The addition of MCO shifted the peak to lower temperatures, for instance, a decrease from  $188.2$  to  $179.4^{\circ}C$  was observed for MNA100 and MNA50:MCO50 samples, respectively. Besides, MNA30:MCO70 and MCO samples shows a decrease in the  $T_p$  of 18.1% and 23.1% respectively. Thus, it is possible to confirm that higher proportion of MCO than MNA provides a significant drop in crosslinking temperature. These results suggest that anhydride group present in MCO has higher reactivity than MNA, indicating faster cure reaction and consequently a possible energy saving in industrial processes. In this regard, Xin et al. studied the curing behavior of epoxy resin with different curing agents such as hexahydrophthalic anhydride (HHPA) and MNA.<sup>56</sup> Despite in this study is not working with long chains of crosslinker such as vegetable oils, it is shown that HHPA, which chemical structure is very similar to anhydride group attach in the MCO molecule, presented higher reactivity than MNA with the corresponding decrease of the peak temperature. Additionally to this effect, the high flexibility provided by aliphatic chains of triglycerides could enable to react easily,<sup>57</sup> thus giving higher reactivity to the anhydride group of bio-based crosslinker.

With regard to enthalpy of crosslinking reaction, it provides the energy released as consequence of curing reaction. In general, the curing reaction in presence of strong Lewis bases such as imidazole involves two steps: the initiation of reaction by means of nucleophilic attack of the nitrogen of 1-methyl imidazole to either anhydride or the epoxy group. This generates an active oxyanion in one end whereas the other functional group is quaternary nitrogen cation.<sup>58</sup> The second step is the propagation, where the active oxyanion could react with the epoxy or anhydride group, being in this case from ECO and MNA and/or MCO, respectively. As a result, an alkoxide or carboxylate anion is formed,<sup>59</sup> respectively, starting the polymerization of ECO and crosslinkers. In this sense, the maximum enthalpy reaction was found to be  $160.9\ J\ g^{-1}$

**TABLE 2** Phase angle ( $\delta$ ) as a function of curing time of ECO crosslinked with different MNA:MCO mixtures obtained by plate-plate oscillatory rheometry

Sample	Crosslinking onset ( $\delta \approx 90^\circ$ ) [s]	Gel time ( $T_g$ ) ( $\delta = 45^\circ$ ) [s]	Crosslinking endset ( $\delta \approx 0^\circ$ ) [s]
<b>MNA100</b>	<b>4854</b>	<b>6225</b>	<b>8639</b>
MNA70:MCO30	1268	1736	3897
MNA50:MCO50	654	865	2195
MNA30:MCO70	221	350	794
MCO100	54	155	663

for MNA100 sample, value that is even higher than commercial epoxy resin-amine reaction ( $140 \text{ J g}^{-1}$ ).<sup>60</sup> Following the same trend as in  $T_p$ , a reduction of area under the curve was observed as MCO content increased. Regarding MCO 100 sample, was possible to observe a sharp decrease of 55.3% of enthalpy compared to MNA100. This reduction is indicating that MCO presents fewer reactive points, that is, less maleated groups per gram taking into account that the molecular weight of MCO is around  $936 \text{ g mol}^{-1}$  compared to  $178.18 \text{ g mol}^{-1}$  of MNA. Similar explanation and finding was reported in the study of ELO with a maximum mixture of MNA and MLO (50:50 wt.%).<sup>41</sup>

Three parameters related to the curing time of all mixtures were measured through plate-plate oscillatory rheometry: (I) the maximum time when the resin stay in liquid state, determined while the  $\delta$  is around  $90^\circ$  due to that when sinusoidal stress is applied to the sample, the elongation/deformation response is delayed  $90^\circ$ , (II) the maximum time for handling the resin, known as gel time ( $T_g$ ) and determined when  $\delta$  is  $45^\circ$  and finally, (III) the time where the crosslinking has been completed and resin behaves as elastic solid, value of  $\delta$  around  $0^\circ$ . Values obtained are summarized in Table 2. The isothermal temperature chosen to develop the assay ( $90^\circ\text{C}$ ), was selected by considering the data obtained by previous assay of DSC. In this assay it is possible to determinate as a minimum of  $90^\circ\text{C}$  is needed to start the crosslinking process. As it is possible to observe, MCO content has notable effect in the crosslinking time. The MNA100 sample needed more than 80 min (4854 s) to start the crosslinking process, while the  $T_g$  was around 103 min (6225 s). MNA 100 sample can be fully crosslinked after 143 min (8639 s). It is worthy to note that with the lowest content of MNA, that is, 70MNA:30MCO sample, these parameters are reduced between a 90–96% respect to sample without the presence of MCO. In the case of sample cured fully with MCO, the descent is more pronounced, giving that is, a  $T_g$  of only 155 s. These values are very close in comparison with the study developed by Fombuena et al. which studied the curing time of commercial

**TABLE 3** Gel content of ECO crosslinked with different MNA:MCO mixtures

Sample	Gel content (%)
<b>MNA100</b>	<b>96.0 <math>\pm</math> 0.09</b>
MNA70:MCO30	97.5 $\pm$ 0.02
MNA50:MCO50	97.5 $\pm$ 0.1
MNA30:MCO70	97.6 $\pm$ 0.02
MCO100	97.9 $\pm$ 0.05

epoxy resin with a minimum biobased content of 55% obtaining a  $T_g$  close to 150 s.<sup>61</sup> These dates are in concordance with values obtained in DSC and corroborate the higher reactivity of MCO compared with the petrochemical anhydride, MNA. Thus, it can conclude that using an isothermal process of  $90^\circ\text{C}$  for 3 h is enough time to crosslink the novel epoxy resins in industrial applications. Moreover, according to literature, post-curing process is recommended in order to ensure that all samples are fully cured as well as improve the mechanical properties. For that reason, the temperature of post curing was  $130^\circ\text{C}$  for 1 extra hour.<sup>62</sup>

### 3.3 | Gel content

The gel content of the different samples has been assessed to study the crosslinking density. All thermosetting samples showed relatively high gel content in the range of 96–97.9% as summarized the Table 3. The lowest gel content value was obtained by MNA100 sample (96.0%), even though the difference is very low compared to other samples (<2%). Therefore, no significant difference is observed between samples that contain MCO as bio-crosslinker and petrochemical crosslinker. Then, it is possible to conclude that MCO addition can increase slightly the crosslinking density, giving well-crosslinked structures. In addition, these high values also indicate that all samples were fully crosslinked with the curing cycle employed for the manufactured thermosetting. It



**FIGURE 5** Visual appearance of ECO crosslinked with different MNA:MCO mixtures after Soxhlet extraction [Color figure can be viewed at [wileyonlinelibrary.com](http://wileyonlinelibrary.com)]

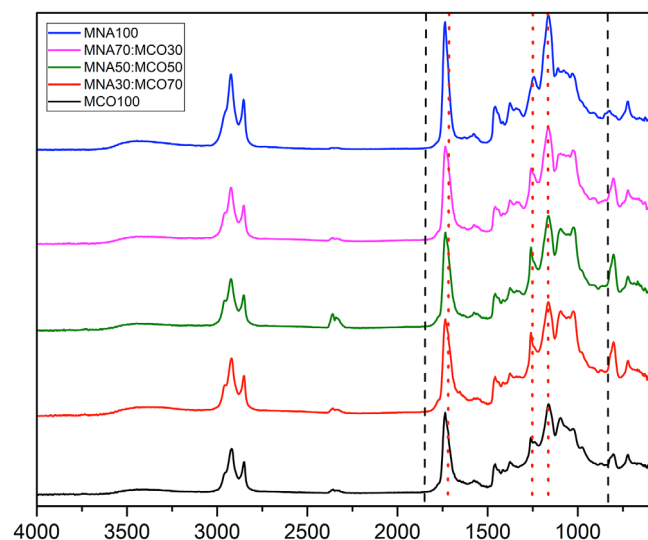
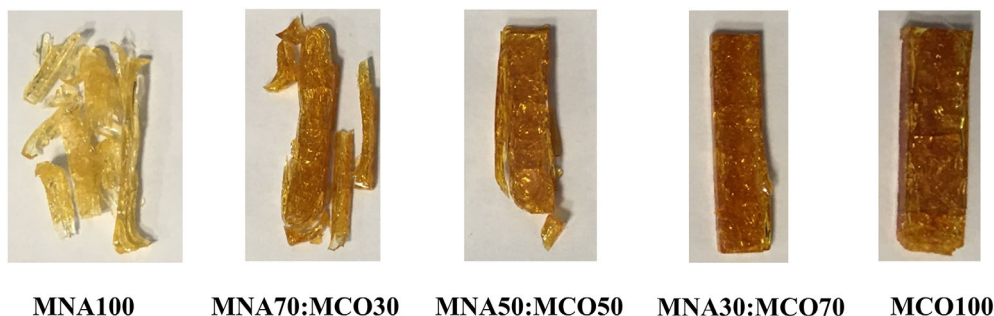


**FIGURE 6** Fourier transform infrared (FT-IR) spectra of cured samples of ECO crosslinked with different MNA:MCO mixtures. [Color figure can be viewed at [wileyonlinelibrary.com](http://wileyonlinelibrary.com)]

should mention that although gel content is similar between samples (1.94% of the difference between them), the physical consistency of the sample after Soxhlet extraction is improved as MCO is added (Figure 5). This fact could be attributed to high crosslinking ability of modified VO during the curing cycle, being in concordance with the high reactivity reported in DSC values.

### 3.4 | Fourier-transformed infrared

The crosslinking reaction was corroborated using FT-IR spectroscopy to confirm the formation of the chemical bonds between epoxy resin (ECO) and crosslinkers (MNA and/or MCO) in cured samples. Figure 6 shows the FT-IR spectra of all samples highlighting the main characteristic peaks. As was commented above in FT-IR of raw materials, the characteristics peaks of functional groups are located at 1859 and 1781  $\text{cm}^{-1}$  for anhydride groups on MNA or MCO structure, and 821  $\text{cm}^{-1}$  for epoxy group on ECO structure. These peaks, highlighted

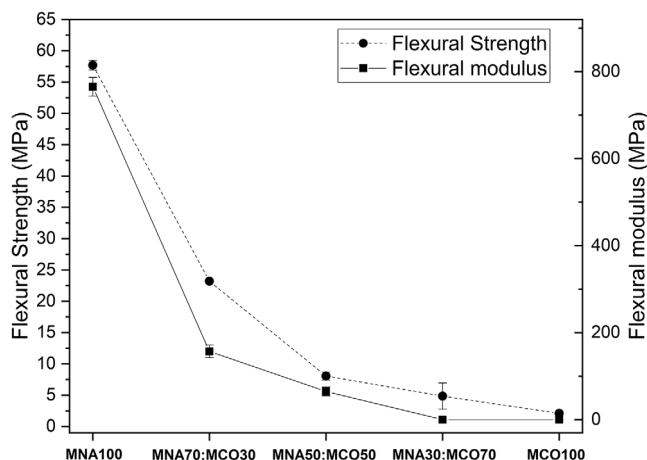


**FIGURE 7** Flexural properties of ECO crosslinked with different MNA:MCO mixtures

in vertical black dashes, disappeared for all samples due to opening of epoxy ring and anhydride groups. Nevertheless, MNA100 sample showed a low intensity peak related to epoxy group (821  $\text{cm}^{-1}$ ), suggesting that not all epoxy groups were opening to interact with the crosslinker. Regarding the main groups that evidence the chemical bonds formed, carbonyl C=O stretching at 1735  $\text{cm}^{-1}$  and C—O—C stretching in the range 1210–1160  $\text{cm}^{-1}$ , have been highlighted with vertical red dots in FT-IR spectra.<sup>63</sup> Therefore, the presence of these peaks confirms the chemical interaction between epoxy resin (ECO) and compatibilizer (MNA and/or MCO).

### 3.5 | Mechanical properties

The effect of bio-based crosslinker (MCO) on the flexural test is shown in Figure 7. First, MNA100 sample showed the highest flexural strength and modulus with values of 57 and 765 MPa, respectively. This sample, with bio-based content of 54.2%, can be compared to other epoxidized VO in literature, taking into account that curing cycle can also affect the final mechanical behavior. Espana et al. obtained values for flexural strength and modulus of 20.7

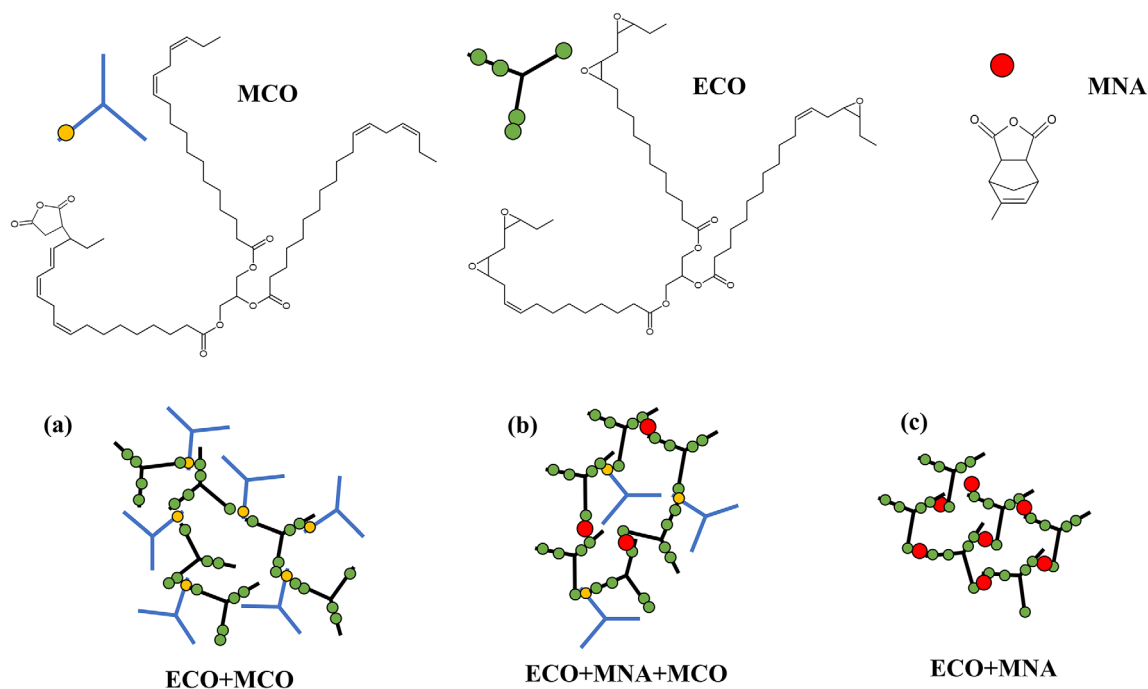


**FIGURE 8** Schematic proposal of polymerization effect of different MNA:MCO mixtures on crosslinked ECO structures [Color figure can be viewed at [wileyonlinelibrary.com](http://wileyonlinelibrary.com)]

and 432 MPa, respectively, using ESO with MNA.<sup>46</sup> On the other side, Samper et al. showed values of 60.8 and 1772.0 MPa for flexural strength and modulus, respectively, using ELO with MNA.<sup>41</sup> These differences with this study can be ascribed to different amount of linkage points of epoxy resins used. In this regard, ECO with EEW (219 g-equiv<sup>-1</sup>) is located between both ESBO and ELO with EEW of 238 and 178 g-equiv<sup>-1</sup>, respectively. Although flexural modulus of ELO was much higher than ECO (1.4 times higher), almost similar values were obtained in terms of tensile strength. In case of the addition of MCO, as greater is the content, the flexural strength and modulus decreases as can be observed, obtaining a more ductile resin. The MNA70:MCO30 sample showed a sharp reduction in both flexural strength and flexural modulus with values of 4.85 and 1.2 MPa, respectively. This behavior is suggesting that MCO presents a high impact in flexural properties in the cured samples. It seems that once MCO is in higher proportion than MNA (from MNA50:MCO50 sample), the properties are kept invariable playing MCO a big role in mechanical properties of the cured samples. It is worthy to note that mechanical properties of samples are strictly related to chemical structure of crosslinker as was observed. Whereas MNA provides a very compact and rigid crosslinking unit,<sup>64</sup> the functionalized long chains of fatty acids lead to increase the free volume and therefore, the chain mobility increase which contributes to improve the flexibility of thermosetting resins.<sup>65</sup> A schematic proposal of polymerization can be seen in Figure 8, where the

**TABLE 4** Influence of cured samples based on ECO crosslinked with different MNA:MCO mixtures in terms of impact-absorbed energy and shore D hardness

Sample	Impact-absorbed energy (kJ m <sup>-2</sup> )	Shore D hardness
MNA100	5.2 ± 0.4	60.9 ± 2.9
MNA70:MCO30	8.4 ± 1.1	50.4 ± 3.9
MNA50:MCO50	12.1 ± 1.1	43.9 ± 3.8
MNA30:MCO70	14.5 ± 2.0	35.7 ± 2.8
MCO100	Didn't break	32.2 ± 2.8

maleated group through -ene reaction is shown even though different modes are also present.

Regarding impact-absorbed energy and Shore D hardness, values are gathered in Table 4. Impact-absorbed energy is related to capacity to absorb energy during an impact. In this regard, MNA 100 sample showed the lowest impact absorption capacity due to its fragile behavior provided by rigid molecule of MNA employed as crosslinker. In the case of bio-based crosslinker, as MCO content increase, higher energy absorbed was obtained due to these samples were more flexible. For instance, an improvement of 181% was achieved with MNA30:MCO70 regarding to MNA100, then obtaining higher ductile properties. The increment of impact-absorbed energy as greater is MCO content can be explained by the presence of long flexible aliphatic chain

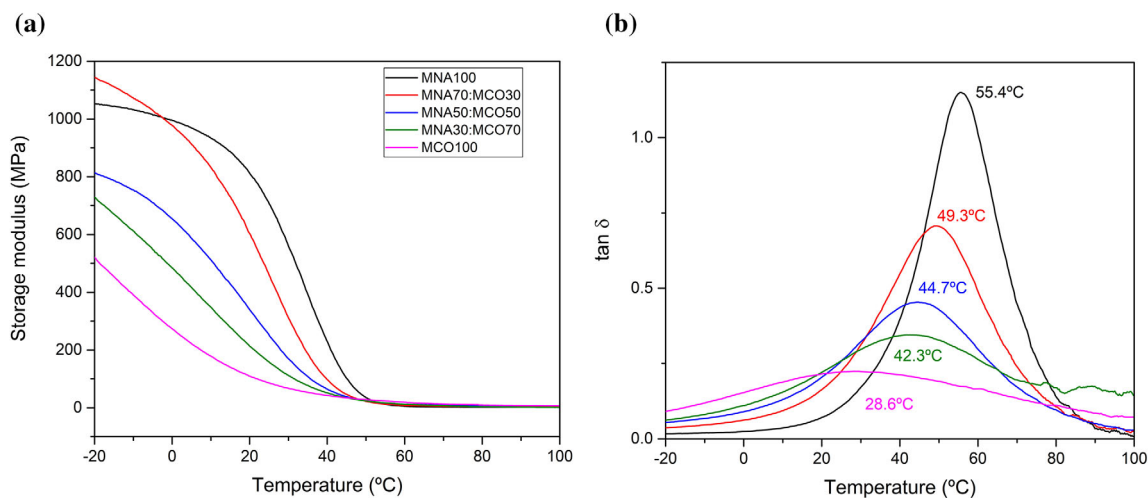


**FIGURE 9** Dynamic mechanical thermal analysis (DMTA) of ECO crosslinked with different MNA:MCO mixtures; (a) storage modulus ( $E'$ ) and (b) damping factor [Color figure can be viewed at [wileyonlinelibrary.com](http://wileyonlinelibrary.com)]

in both ECO and MCO. Similar explanation and finding were reported for epoxy blends with ELO and petroleum epoxy resin with cardanol-derived phenalkamine (PKA).<sup>66</sup> Regarding to MCO100 sample, the deformation took place but not break was obtained during this test, meaning that whole energy of impact was absorbed by the sample. This behavior was also observed by Espana et al. who studied ESBO with MNA in ratio of 1:0.7 (EEW:AEW).<sup>46</sup> On contrary, Shore D hardness values decreased from 60.9 to 32.2 for MNA100 and MCO100 sample, respectively, in consequence of more ductile behavior. The addition of MCO as bio-based crosslinker led to obtain less compact structure for the increment of free volume provided by the long chains of MCO, thus reducing the hardness of cured sample. Moreover, these values are in concordance with flexural tests, which corroborates that addition of MCO contributes to increase the flexibility. As one can observe, depending on formulation, it is possible to manufacture thermosetting samples with wide range of mechanical properties from high rigidity to high ductility with bio-based content up to 98%.

The thermomechanical performance of the samples was analyzed by DMTA. In Figure 9 is shown the storage modulus ( $E'$ ) and damping factor ( $\tan \delta$ ) curves as a function of temperature. Concerning  $E'$ , MNA100 sample reported a value of 820 MPa at room temperature (20°C), which value is close to the obtained with ELO crosslinked with MNA.<sup>41</sup> In general, with increasing MCO content,  $E'$  decreases gradually from 820 MPa to 100 MPa at room temperature for MNA 100 and MCO 100 sample, respectively, indicating a change of behavior from rigid to flexible materials. These values are in concordance with the mechanical properties obtained above, where

long chains of MCO provide more flexibility to cured samples and then, it results in lower  $E'$ . In relation to the damping factor, this value provides information to estimate the  $T_g$  of the samples. It was observed that as increased the MCO content,  $T_g$  values decreased even though with a different peak shape. This trend was also expected as a result of flexibility provided by MCO as bio-based crosslinker. For example, MNA100 sample exhibit a narrow peak curve with  $T_g$  value of 55.4°C, whereas it becomes broader and less intense gradually as increase the MCO content up to values of 28.6°C for MCO100 sample. It is known that the dynamic mechanical properties of thermosetting depend on the composition and chemical structure.<sup>67</sup> In this regard, the rigid structure of MNA presents a small free volume that hinders the movement of molecular chains at lower temperature, only increasing the free volume as temperature arises in order to procedure the glass transition (narrow peak). On contrary, MCO contains a flexible structure with high free volume that ease the movement of molecular chains at lower temperature, which results in a wider peak with less intensity as MCO content increases.

### 3.6 | Morphology of cured samples

To reveal the effect of the incorporation of MCO as crosslinker and consequently the relationship between the mechanical behavior of the resins developed with the morphology of the fractured surface, an analysis by SEM were carried out as shown in Figure 10. The sample fractured of ECO crosslinked with 100 MNA showed a typical morphology for rigid and fragile materials characterized by homogenous and smooth surface, Figure 10a.

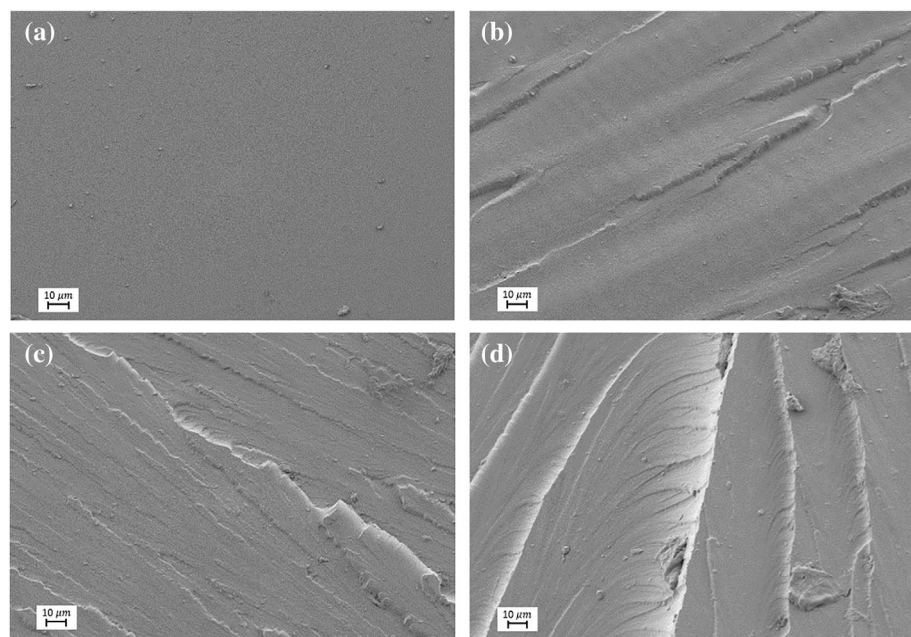


**FIGURE 10** SEM images of fractured samples of crosslinked ECO with different MNA:MCO mixtures at 500 $\times$ : (a) MNA100, (b) MNA70:MCO30, (c) MNA50:MCO50 and (d) MNA70:MCO30

In this regard, the typical waves were not observed due to high fragility of sample. Similar fragile surface has been reported in thermosetting resins of ELO and MNA.<sup>68</sup> As was expected, the addition of MCO gave rougher surface with an evident multiple microcracks advancing in direction of the break. With regard to MNA70:MCO30 sample, it becomes to display a small and low presence of crests as well as a remaining smooth surface, Figure 10b. This fractured surface indicates an improvement of toughness properties.<sup>69</sup> As increase MCO content (MNA50:50MCO sample), an increment of both size and number of waves were observed. It is remarkable that from this formulation onwards, the mechanical properties such as flexural and absorbed energy, become to reach a plateau what can be ascribed to the presence of this specific fractured surface. In case of the highest MCO content fracture surface (MNA30:MCO70), a continuous advancing front of cracks with rippled edges were observed in Figure 10d that confirms the highest toughening behavior after cracking. In addition, no obvious phase separation was observed in all samples neither with MNA nor mixtures with MNA and MCO, which indicates a good compatibility with homogenous crosslinking network. This is an advantage compared to some authors where observed a phase separation in mixtures with ESO and glycerol or pentaerythritol based aliphatic epoxy resin from renewable sources.<sup>45</sup>

#### 4 | CONCLUSION

Novel epoxy resins based on ECO as bio-based epoxy matrix has been assessed with different crosslinkers

mixtures (MNA and/or MCO). The main functional groups of raw materials were identified by means of titration method and FT-IR, especially for ECO and MCO that were obtained through chemical modification from CO with the aim to be employed for the first time in thermosetting resins. Besides, the success of the reaction of MCO was characterized for the first time using <sup>1</sup>H NMR spectroscopy with AEW of 841 g-equiv<sup>-1</sup>. According to our DSC results, all samples start to cure around 80°C and finish in the range of 230–240°C. Furthermore, the addition of MCO leads to shift the temperature of exothermic curing peak to lower temperatures from 188.2°C for 100MNA sample to 144.9°C for 100MCO sample, indicating higher reactivity of MCO compared to MNA. The isothermal curing at 90°C in plate-plate oscillatory rheometer also corroborated the higher reactivity of MCO achieving a gel time of 150 s for sample fully cured with MCO (100MCO sample) with a high bio-based content of 98%. These values are found to be very close to cured samples with commercial epoxy resin with low-medium bio-based content of 55%. This faster curing compared to MNA could mean a possible energy saving from industrial point of view. All cured samples had high gel contents of about 96%–97.9%, which indicates well-crosslinked structures. In addition, FT-IR of cured samples demonstrates the chemical interaction of ECO and MNA/MCO. In terms of mechanical properties, the addition of MCO provides more flexibility, thus increasing the impact-absorbed energy and decreasing the flexural properties and shore D values. A similar trend was observed in DMTA analysis with a decrease of E' from 820 to 100 MPa at room temperature and T<sub>g</sub> from 55.4 to 28.6°C as greater is the addition of MCO. The T<sub>g</sub> of



100MCO (28.6°C) was much higher than reported in literature for commercial ECO and MCO cured sample with  $T_g$  value of  $-41^\circ\text{C}$ . The mechanical behavior was corroborated by SEM images of fractured samples, which showed a rough surface as MCO content increased, giving more ductility to the thermosetting resins. Therefore, by adding the adequate amount of MCO as bio-based crosslinker, it is possible to tailor the desired thermal and mechanical properties of thermosetting resins based on ECO, improving the ductility, and curing time. In addition to this wide range of properties, from environmental point of view, the bio-based content of cured resins is in the range of 54.2%–98%, thus giving a noticeable feature to these green epoxy resins even reaching almost fully bio-based content (98%) using only MCO as bio-renewable crosslinker.

### AUTHOR CONTRIBUTIONS

**Ivan Dominguez-Candela:** Conceptualization; investigation; methodology and writing-original draft preparation; **Aina Perez-Nakai:** Formal analysis; data curation and validation; **Elena Torres-Roca:** Formal analysis; data curation and methodology; **Jaime Lora-Garcia:** Resources; visualization; supervision and project administration; **Vicent Fombuena:** Conceptualization; resources; writing-reviewing and editing; supervision and project administration.

### ACKNOWLEDGMENTS

This research work was funded by the Ministry of Science and Innovation—"Retos de la Sociedad". Project references: PID2020-119142RA-I00. I. Dominguez-Candela wants to thank Universitat Politècnica de València for his FPI grant (PAID-2019-SP20190013) and Generalitat Valenciana-GVA (ACIF/2020/233). Funding for open access charge: CRUE-Universitat Politècnica de València.

### DATA AVAILABILITY STATEMENT

Research data are not shared.

### ORCID

Ivan Dominguez-Candela  <https://orcid.org/0000-0003-3288-1079>

### REFERENCES

- [1] M. N. Belgacem, A. Gandini, *Monomers, Polymers and Composites from Renewable Resources*, Elsevier, Oxford, **2008**, p. 1.
- [2] C. K. Williams, M. A. Hillmyer, *Polym. Rev.* **2008**, *48*, 1.
- [3] P. J. Halley, R. W. Truss, M. G. Markotsis, C. Chaleat, M. Russo, A. L. Sargent, I. Tan, P. A. Sopade, A Review of Biodegradable Thermoplastic Starch Polymers. Proceedings of the Symposium on Polymer Performance and Degradation held at Pacificchem 2005 Conference, Honolulu, HI, **2005**; pp. 287–300.
- [4] A. Chakrabarty, Y. Teramoto, *Polymer* **2018**, *10*, 517. <https://doi.org/10.3390/polym10050517>
- [5] M. Parit, Z. Jiang, *Int. J. Biol. Macromol.* **2020**, *165*, 3180.
- [6] D. Garcia-Garcia, L. Quiles-Carrillo, N. Montanes, V. Fombuena, R. Balart, *Materials* **2018**, *11*, 35. <https://doi.org/10.3390/ma11010035>
- [7] A. Qurat ul, K. M. Zia, F. Zia, M. Ali, S. Rehman, M. Zuber, *Int. J. Biol. Macromol.* **2016**, *93*, 1057.
- [8] X. He, G. Wu, Y. Yan, *Sheng wu Gong cheng Xue bao Chin. J. Biotechnol.* **2017**, *33*, 701.
- [9] P. Anastas, N. Eghbali, *Chem. Soc. Rev.* **2010**, *39*, 301.
- [10] J. Carlos Ronda, G. Lligadas, M. Galia, V. Cadiz, *Eur. J. Lipid Sci. Technol.* **2011**, *113*, 46.
- [11] G. Lligadas, J. C. Ronda, M. Galia, V. Cadiz, *Mater. Today* **2013**, *16*, 337.
- [12] G. A. Smith, *J. Am. Oil Chem. Soc.* **2020**, *97*, 32.
- [13] N. A. Masripan, M. A. Salim, G. Omar, M. R. Mansor, A. M. Saad, N. A. Hamid, M. I. Syakir, F. Dai, *Int. J. Nanoelectron. Mater.* **2020**, *13*, 161.
- [14] P. Jia, H. Xia, K. Tang, Y. Zhou, *Polymer* **2018**, *10*, 1303. <https://doi.org/10.3390/polym10121303>
- [15] C. Burgos-Diaz, T. Wandersleben, A. M. Marques, M. Rubilar, *Curr. Opin. Colloid Interface Sci.* **2016**, *25*, 51.
- [16] S. N. H. Mustapha, A. R. Rahmat, A. Arsad, *Rev. Chem. Eng.* **2014**, *30*, 167.
- [17] A. H. M. Azam, T. Sarmidi, A. S. M. Nor, M. Zainuddin, *Int. J. Bus. Soc.* **2020**, *21*, 1068.
- [18] N. Karak, *Vegetable Oil-Based Polymer Composites*, Elsevier, Amsterdam, Netherlands, **2012**, pp. 247–270.
- [19] M. Zuk, D. Richter, J. Matula, J. Szopa, *Ind. Crops Prod.* **2015**, *75*, 165.
- [20] H. Barcena, A. Tuachi, Y. Z. Zhang, *J. Chem. Educ.* **2017**, *94*, 1314.
- [21] B. Matthaus, L. Bruhl, *Eur. J. Lipid Sci. Technol.* **2008**, *110*, 655.
- [22] H. Harish, S. Rajanna, G. S. Prakash, S. M. Ahamed, Extraction of biodiesel from tung seed oil and evaluating the performance and emission studies on 4-stroke CI engine. Proceedings of the 4th International Conference on Advances in Materials and Manufacturing Applications (ICONAMMA), India, Aug 29–31, **2019**, pp. 4869–4877.
- [23] I. Dominguez-Candela, A. Lerma-Canto, S. C. Cardona, J. Lora, V. Fombuena, *Materials* **2022**, *15*, 3250. <https://doi.org/10.3390/ma15093250>
- [24] Chia Seeds Market SizeWorth \$4.7 Billion by 2025. Available online: (accessed on).
- [25] Z. S. Petrovic, A. Zlatanic, C. C. Lava, S. Sinadinovic-Fiser, *Eur. J. Lipid Sci. Technol.* **2002**, *104*, 293.
- [26] A. Carbonell-Verdu, D. Garcia-Sanoguera, A. Jorda-Vilaplana, L. Sanchez-Nacher, R. Balart, *J. Appl. Polym. Sci.* **2016**, *133*, 43642. <https://doi.org/10.1002/app.43924>
- [27] O. Fenollar, D. Garcia-Sanoguera, L. Sanchez-Nacher, J. Lopez, R. Balart, *J. Appl. Polym. Sci.* **2012**, *124*, 2550.
- [28] M. Li, S. H. Li, J. L. Xia, C. X. Ding, M. Wang, L. N. Xu, X. H. Yang, K. Huang, *Mater. Des.* **2017**, *122*, 366.
- [29] M. T. Taghizadeh, N. Nalbandi, A. Bahadori, *Express Polym. Lett.* **2008**, *2*, 65.

- [30] V. Fombuena, R. Petrucci, F. Dominici, A. Jorda-Vilaplana, N. Montanes, L. Torre, *Polymer* **2019**, *11*, 18.
- [31] C. Ding, A. S. Matharu, *ACS Sustain. Chem. Eng.* **2014**, *2*, 2217.
- [32] M. D. Samper, R. Petrucci, L. Sanchez-Nacher, R. Balart, J. M. Kenny, *Compos. Part B Eng.* **2015**, *71*, 203.
- [33] C. F. Frias, A. C. Serra, A. Ramalho, J. F. J. Coelho, A. C. Fonseca, *Ind. Crops Prod.* **2017**, *109*, 434.
- [34] S. Zhang, T. Liu, C. Hao, A. Mikkelsen, B. Zhao, J. Zhang, *ACS Sustain. Chem. Eng.* **2020**, *8*, 14964.
- [35] *Epoxy Resins and Curing Agents: Toxicology, Health, Safety and Environmental Aspects*, Plastics Europe Epoxy Resins Committee, Brussels, Belgium **2006**, p. 1.
- [36] *Cyclic Acid Anhydrides: Health-Based Recommended Occupational Exposure Limit*; **2010**.
- [37] M. Stemmelen, F. Pessel, V. Lapinte, S. Caillol, J. P. Habas, J. J. Robin, *J. Polym. Sci. Part A-Polym. Chem.* **2011**, *49*, 2434.
- [38] M. Stemmelen, V. Lapinte, J.-P. Habas, J.-J. Robin, *Eur. Polym. J.* **2015**, *68*, 536.
- [39] H. Warth, R. Mulhaupt, B. Hoffmann, S. Lawson, *Angew. Makromol. Chem.* **1997**, *249*, 79.
- [40] T. Takahashi, K.-I. Hirayama, N. Teramoto, M. Shibata, *J. Appl. Polym. Sci.* **2008**, *108*, 1596.
- [41] M. D. Samper, J. M. Ferri, A. Carbonell-Verdu, R. Balart, O. Fenollar, *Express Polym. Lett.* **2019**, *13*, 407.
- [42] I. Dominguez-Candela, J. M. Ferri, S. C. Cardona, J. Lora, V. Fombuena, *Polymer* **2021**, *13*, 16.
- [43] A. Lerma-Canto, J. Gomez-Caturula, M. Herrero-Herrero, D. Garcia-Garcia, V. Fombuena, *Polymer* **2021**, *13*, 1392. <https://doi.org/10.3390/polym13091392>
- [44] B. Ellis, *Chemistry and Technology of Epoxy Resins*, Springer, London, **1993**.
- [45] P. Niedermann, G. Szebenyi, A. Toldy, *J. Polym. Environ.* **2014**, *22*, 525.
- [46] J. M. Espana, L. Sanchez-Nacher, T. Boronat, V. Fombuena, R. Balart, *J. Am. Oil Chem. Soc.* **2012**, *89*, 2067.
- [47] A. Ito, T. Semba, K. Taki, M. Ohshima, *J. Appl. Polym. Sci.* **2014**, *131*, 40407. <https://doi.org/10.1002/app.40407>
- [48] J. R. Kim, S. Sharma, *Ind. Crops Prod.* **2012**, *36*, 485.
- [49] L. Quiles-Carrillo, M. M. Blanes-Martinez, N. Montanes, O. Fenollar, S. Torres-Giner, R. Balart, *Eur. Polym. J.* **2018**, *98*, 402.
- [50] L. Candy, C. Vaca-Garcia, E. Borredon, *J. Am. Oil Chem. Soc.* **2005**, *82*, 271.
- [51] C. Gaglieri, R. T. Alarcon, A. de Moura, R. Magri, L. C. da Silva-Filho, G. Bannach, *J. Braz. Chem. Soc.* **2021**, *32*, 2120.
- [52] E. Lackinger, L. Schmid, J. Sartori, A. Isogai, A. Potthast, T. Rosenau, *Holzforchung* **2011**, *65*, 3.
- [53] R. Vendamme, K. Olaerts, M. Gomes, M. Degens, T. Shigematsu, W. Eevers, *Biomacromolecules* **2012**, *13*, 1933.
- [54] R. C. Amos, M. Kuska, J. Mesnager, M. Gauthier, *Ind. Crops Prod.* **2021**, *166*, 113504.
- [55] W. Chen, P. Li, Y. Yu, X. Yang, *J. Appl. Polym. Sci.* **2008**, *107*, 1493.
- [56] J. Xin, P. Zhang, K. Huang, J. Zhang, *Rsc Adv.* **2014**, *4*, 8525.
- [57] K. Huang, P. Zhang, J. Zhang, S. Li, M. Li, J. Xia, Y. Zhou, *Green Chem.* **2013**, *15*, 2466.
- [58] S. Kumar, S. K. Samal, S. Mohanty, S. K. Nayak, *Thermochim. Acta* **2017**, *654*, 112.
- [59] A. Paramarta, D. C. Webster, *React. Funct. Polym.* **2016**, *105*, 140.
- [60] H. A. Shnawa, *Polym. Bull.* **2021**, *78*, 1925.
- [61] V. Fombuena, L. Bernardi, O. Fenollar, T. Boronat, R. Balart, *Mater. Des.* **2014**, *57*, 168.
- [62] C. H. Lin, C. Y. Wu, C. S. Wang, *J. Appl. Polym. Sci.* **2000**, *78*, 228.
- [63] A. Marotta, N. Faggio, V. Ambrogi, P. Cerruti, G. Gentile, A. Mija, *Biomacromolecules* **2019**, *20*, 3831.
- [64] G. Ragosta, P. Musto, G. Scarinzi, L. Mascia, *Polymer* **2003**, *44*, 2081.
- [65] B. De, K. Gupta, M. Mandal, N. Karak, *ACS Sustain Chem. Eng.* **2014**, *2*, 445.
- [66] S. K. Sahoo, V. Khandelwal, G. Manik, *Polym. Adv. Technol.* **2018**, *29*, 565.
- [67] S. Wang, J. L. Wang, Q. Ji, A. R. Shultz, T. C. Ward, J. E. McGrath, *J. Polym. Sci. Part B Polym. Phys.* **2000**, *38*, 2409.
- [68] M. D. Samper, V. Fombuena, T. Boronat, D. Garcia-Sanoguera, R. Balart, *J. Am. Oil Chem. Soc.* **2012**, *89*, 1521.
- [69] H. Miyagawa, A. K. Mohanty, M. Misra, L. T. Drzal, *Macromol. Mater. Eng.* **2004**, *289*, 629.

**How to cite this article:** I. Dominguez-Candela, A. Perez-Nakai, E. Torres-Roca, J. Lora-Garcia, V. Fombuena, *J. Appl. Polym. Sci.* **2022**, e53574. <https://doi.org/10.1002/app.53574>